This is a repository copy of *Constraints on late time violations of the equivalence principle in the dark sector*.

White Rose Research Online URL for this paper:
https://eprints.whiterose.ac.uk/198307/

Version: Published Version

Constraints on late time violations of the equivalence principle in the dark sector

To cite this article: Cameron C. Thomas and Carsten van de Bruck JCAP04(2023)015

View the article online for updates and enhancements.

Constraints on late time violations of the equivalence principle in the dark sector

Cameron C. Thomas and Carsten van de Bruck

Consortium for Fundamental Physics, School of Mathematics and Statistics,
University of Sheffield,
Hounsfield Road, Sheffield S3 7RH, U.K.

E-mail: ccthomas2@sheffield.ac.uk, c.vandebruck@sheffield.ac.uk

Abstract. If dark energy is dynamical due to the evolution of a scalar field, then in general it is expected that the scalar is coupled to matter. While couplings to the standard model particles are highly constrained by local experiments, bounds on couplings to dark matter (DM) are only obtained from cosmological observations and they are consequently weaker. It has recently been pointed out that the coupling itself can become non-zero only at the time of dark energy domination, due to the evolution of dark energy itself, leading to a violation of the equivalence principle (EP) in the dark sector at late times. In this paper we study a specific model and show that such late-time violations of the EP in the DM sector are not strongly constrained by the evolution of the cosmological background and by observables in the linear regime (e.g. from the cosmic microwave background radiation), although the model is not preferred over ΛCDM. A study of perturbations in non-linear regime is necessary to constrain late-time violations of the equivalence principle much more strongly.

Contents

1 Introduction

There are several reasons to study alternative theories to the cosmological constant as a model for dark energy (DE). Firstly, if DE is due to a non-vanishing cosmological constant, its value has to be very small to fit the data. The expected theoretical value, however, is much larger. This problem has not been solved, but there are attempts to address this problem (see [1–3] and references therein). Secondly, there are several tensions between data sets, providing tantalising hints that the standard model of cosmology, the Λ-Cold-Dark-Matter(ΛCDM) model, may be in need of corrections. For example, measurements of the expansion rate of the universe today, the Hubble constant, using the cosmic microwave background radiation (CMB) or using inferred distances in the late universe do not agree with a high statistical significance. Another tension is related with the amplitude of clustering of matter in the late Universe. The distribution of galaxies and matter in the late Universe is smoother than predicted in the ΛCDM model. We refer to [4] for a recent overview of the tensions and [5, 6] for overviews of attempts to solve the tensions.

Among the extensions of the ΛCDM model which remain the best motivated ones are scalar-field models of DE, in which the accelerated expansion is driven by a scalar field [7–9]. Some dynamical dark energy models are motivated specifically to address the tensions mentioned above [10, 11]. It is expected that, in general, the scalar is coupled to at least one species of matter, unless there is a symmetry which forbids such couplings [12]. Such a coupling results in an additional force mediated between the coupled species. Since the interaction between DE and ordinary matter is strongly constrained, in some models only the coupling to cold dark matter (CDM) is of cosmological significance (see e.g. [13–17] and references therein). It is this type of theory which we consider in this paper.

It has recently been suggested that the potential energy of scalar fields appearing in string theory cannot be arbitrarily flat [18, 19], see [20] for an overview of the swampland programme. If true, the accelerated expansion cannot be driven by a cosmological constant (de Sitter space is not realised in string theory) and the equation of state of dark energy is not constant and deviates potentially significantly from the value expected in the ΛCDM model. Additionally, a coupling of the scalar to some sectors in the theory are expected. Based on these observations, several phenomenological models have been proposed recently [21–26]. In this paper we study specific a model in which the coupling function between the dark energy field and dark matter has a minimum [21]. As a result of the minimum, the coupling switches on only at late times, at the beginning of the dark energy dominated epoch. One of our main results of this paper is that the regime in which linear perturbation theory is

valid does not constrain the conformal coupling parameter of the model greatly. In other words, late time violations of the equivalence principle in the dark sector are not strongly constrained by studying the background evolution or CMB anisotropies. Instead, to obtain stronger constraints a study of the non-linear regime in considerable detail is needed.

The paper is organised as follows. In section 2 we present the model and its parameters. In section 3 we describe our methodology, describe the data sets used and present the constraints on the model. We conclude in section 4.

2 Interacting dark energy

The model we consider consists of the gravitational sector described by the Einstein-Hilbert action without cosmological constant, a part which describes the standard model (SM) particles and a part for DE described by a scalar field ϕ with potential energy $V(\phi)$. Finally, the interaction between DE and DM is described by a conformal coupling. The full action reads

$$
\mathcal{S} = \int d^4x \sqrt{-g} \left(\frac{M_{\rm Pl}^2}{2} \mathcal{R} - \frac{1}{2} g^{\mu\nu} \partial_\mu \phi \partial_\nu \phi - V(\phi) \right)
$$
$$
+ \int d^4x \sqrt{-g} \mathcal{L}_{\rm SM}(g, \Psi_i) + \int d^4x \sqrt{-\tilde{g}} \mathcal{L}_{\rm DM}(\tilde{g}, \chi) \tag{2.1}
$$

where $M_{\rm Pl}$ is the reduced Planck mass, $\mathcal{R}$ is the Ricci-scalar, the SM fields are denoted by Ψ_i and χ is the DM field (assuming here for simplicity that dark matter consists of only one species). The metrics g and $\tilde{g}$ are related by a conformal transformation $\tilde{g}_{\mu\nu} = C(\phi)g_{\mu\nu}$. Such theories have been discussed in considerable length in the literature, but the new ingredient in this paper is that the function $C(\phi)$ has a minimum. That the coupling functions in string theory could possess a minimum due to non-perturbative effects was suggested in the works by Damour and Polyakov [27] and has been used in [28] to construct a dilaton-model of DE. Combining these theoretical developments motivated us in [21] to consider a specific model in which $C(\phi)$ has a minimum at some scalar field value ϕ_*. To be concrete, in this paper we consider the following function for $C(\phi)$:

$$
C(\phi) = \cosh\left(\sqrt{\alpha}\, (\phi - \phi_*)/M_{\rm Pl} \right), \tag{2.2}
$$

where ϕ_* denotes the minimum of the function $C(\phi)$ and α is a constant. In this paper we choose $\phi_* = 1\, M_{\rm Pl}$ without loss of generality. In [21] it was pointed out that even if the field starts away from the minimum in the very early universe, there are attractor mechanisms at work in the early universe which drive the field towards the minimum quickly. Nevertheless, in our analysis below we allow the field to start away from the minimum value at ϕ_* to find constraints on the initial conditions of the DE field. In our analysis we choose an exponential potential with

$$
V(\phi) = V_0 e^{-\lambda \phi/M_{\rm Pl}}, \tag{2.3}
$$

where λ denotes the slope of the potential, which in string theory according to [18] cannot be arbitrarily small and should be $\mathcal{O}(1)$. Finally, we assume in the following that the universe is spatially flat.

Because of the coupling, there is an exchange of energy between DM and the DE field. As a result, the evolution of the DM density and the modified Klein-Gordon equation are given by

$$
\dot{\rho}_{\rm DM} + 3H\rho_{\rm DM} = \beta M_{\rm Pl}^{-1} \dot{\phi} \rho_{\rm DM}
$$
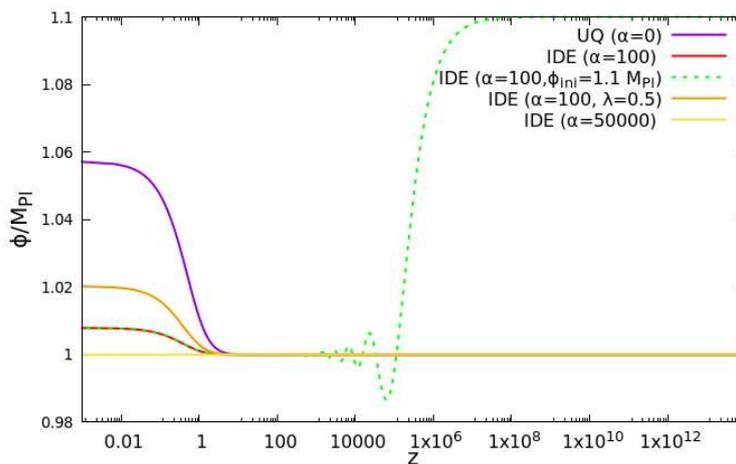
Figure 1. Evolution of the scalar field in units $M_{\rm Pl}$ for IDE models with a variety of values of α, λ, and $\phi_{\rm ini}$, where the uncoupled quintessence (UQ) model is given by imposing $\alpha = 0$ on the IDE model. The slope of the scalar field potential is set to $\lambda = 0.2$ in all the models unless specified otherwise. Where applicable, the values of the cosmological parameters used are derived from a ΛCDM cosmology using *Planck* TTTEEE+lowE [29].

and

$$\ddot{\phi} + 3H\dot{\phi} + V_\phi = -\beta M_{\rm Pl}^{-1}\rho_{\rm DM}.$$

In these equations we have defined

$$\beta = \frac{M_{\rm Pl}}{2}\frac{{\rm d}\ln C}{{\rm d}\phi}, \tag{2.4}$$

which for the coupling considered in this paper (eq. (2.2)) is

$$\beta = \frac{\sqrt{\alpha}}{2}\tanh\left(\sqrt{\alpha}\left(\phi - \phi_*\right)/M_{\rm Pl}\right). \tag{2.5}$$

The effective gravitational constant between two DM particles is given by [21, 30]

$$G_{\rm eff} = G_N\left(1 + 2\beta^2\right). \tag{2.6}$$

In figure 1 we plot the evolution of the scalar field for different values of coupling parameter α, slope of potential λ, and value of scalar field at $a = 10^{-14}$ when simulations start, $\phi_{\rm ini}$, for the interacting dark energy (IDE) model. We see from this plot that the coupling inhibits the evolution of ϕ at late-times, with the field traversing a shorter distance the larger the value of the coupling constant α. When the field is initially displaced from the minimum, it is driven towards the minimum as the matter energy density becomes dynamically important, after which its evolution closely follows the case where the field initially sits at the minimum. Finally, we see that increasing the steepness of the potential, λ, causes the field to roll further at late-times.

The evolution of $G_{\rm eff}$ is shown in figure 2 for various choices of parameters α and λ. If the field initially sits at the minimum of the coupling ϕ_*, the additional force between DM particles due to the scalar field only becomes significant at redshifts $z \lesssim 1$, when the DE field starts to evolve due to the influence of the potential. If the field is initially displaced

– 3 –
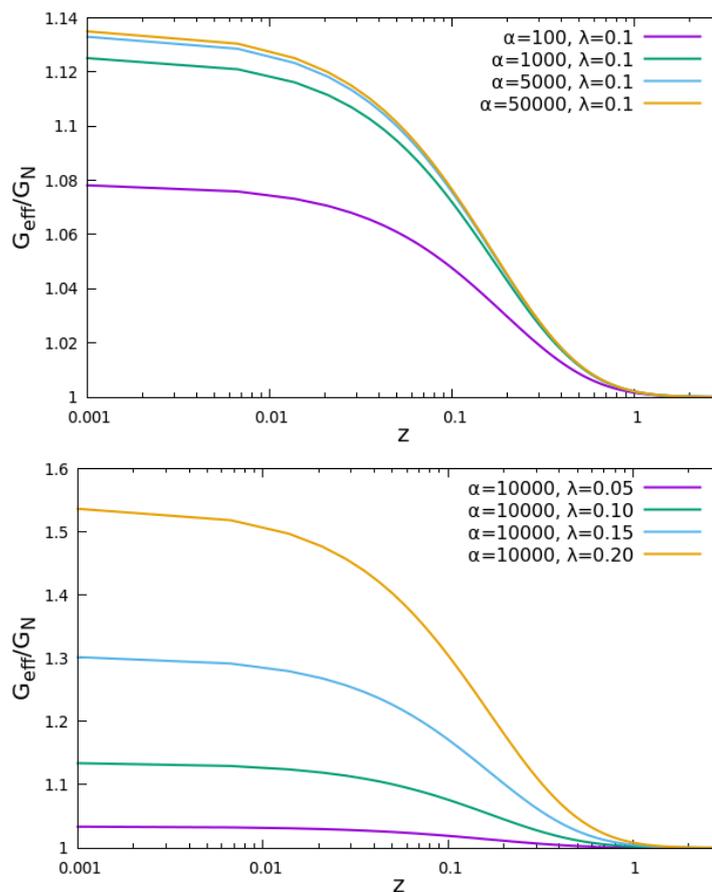
Figure 2. Evolution of the effective gravitational constant, defined in eq. (2.6), for models with a different value of α but same value of $\lambda = 0.1$ (top) and for models with a different value of λ but same value of $10^{-4}\alpha = 1$ (bottom). Where applicable, the values of the cosmological parameters used are derived from a ΛCDM cosmology using *Planck* TTTEEE+lowE [29].

from the minimum, then there exists a fifth-force between DM particles which vanishes as the matter energy density becomes important as can be seen in figure 1. We emphasise that the effective gravitational coupling (eq. (2.6)) between DM particles depends on α as well as the distance between the scalar field and minimum ϕ_*.

We plot the percentage difference of the CMB temperature anisotropy power spectrum with respect to ΛCDM and the percentage difference of the matter power spectrum with respect to ΛCDM in the upper and lower panel of figure 3 respectively. We see in these plots that even for large values of coupling constant α, the deviation with respect to ΛCDM remains fairly minimal, however, that increasing the slope of the potential λ has a more notable effect. Turning our attention to the lower panel of figure 3, we see a significant deviation from ΛCDM for the case where the field does not initially sit at the minimum. This enhancement in power at small to intermediate scales is due to an early-time enhancement in the effective gravitational constant between DM particles, G_{eff}.

To summarise, the parameters of the model we seek to constrain are the slope of the potential λ, the coupling parameter α, which is related to strength of the coupling between DM and DE, and the initial field value ϕ_{ini} deep inside the radiation dominated epoch.
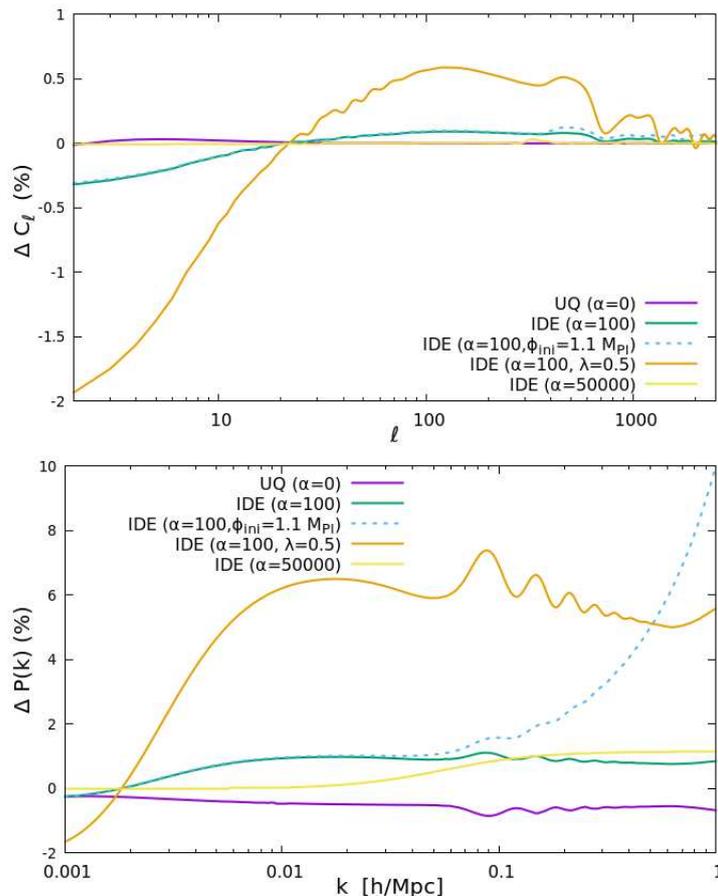
Figure 3. *Upper panel*: percentage difference of the CMB temperature anisotropy power spectrum for a model i with respect to the ΛCDM model, where $\Delta C_\ell = C_{\ell,i}/C_{\ell,\Lambda\text{CDM}} - 1$. *Lower panel*: percentage difference of the present-day matter power spectrum for a model i with respect to the ΛCDM model, where $\Delta P(k) = P(k)_i/P(k)_{\Lambda\text{CDM}} - 1$. The slope of the scalar field potential is set to $\lambda = 0.2$ in all the models unless specified otherwise.

3   Methodology, data and results

In our analysis, the IDE model is described by a set of nine parameters whose priors are specified in table 1 and where h is the reduced Hubble constant defined by $H_0 = 100h\,\text{km}\,\text{s}^{-1}\,\text{Mpc}^{-1}$. These parameters are the reduced baryon energy density $\Omega_b h^2$, the reduced CDM energy density $\Omega_{\text{cdm}} h^2$, the ratio of the sound horizon to the angular diameter distance at decoupling θ_s, the scalar amplitude of the primordial power spectrum A_s, the scalar spectral index n_s, the reionisation optical depth τ_{reio}, the slope of the scalar field potential λ, the conformal coupling parameter α, and the initial value of the scalar field ϕ_{ini}.

In order to numerically study the evolution of the background and cosmological perturbations for the IDE model described above, we use a modified version of the `CLASS`[1] code [31, 32]. For cosmological parameter exploration, we use the Markov Chain Monte Carlo (MCMC) sampling package `MontePython`[2] [33, 34] in conjunction with the data sets

---

[1]https://github.com/lesgourg/class_public.

[2]https://github.com/brinckmann/montepython_public.

Parameter	Prior
$\Omega_b h^2$	$[0.005, 0.1]$
$\Omega_{\mathrm{cdm}} h^2$	$[0.001, 0.99]$
$100\theta_s$	$[0.5, 10.0]$
$\ln\left(10^{10} A_s\right)$	$[2.7, 4.0]$
n_s	$[0.9, 1.1]$
τ_{reio}	$[0.01, 0.8]$
λ	$[0, 2]$
$10^{-4}\alpha$	$[0, 50]$
$\phi_{\mathrm{ini}}/M_{\mathrm{Pl}}$	$[0, 2]$

Table 1. Flat priors for the cosmological parameters sampled in our analysis.

Parameter	ΛCDM	IDE	IDE $(\phi_{\mathrm{ini}} = 1M_{\mathrm{Pl}})$	Uncoupled quintessence $(\alpha = 0)$
$\Omega_b h^2$	0.02247 ± 0.00013	0.02247 ± 0.00013	0.02246 ± 0.00013	0.02248 ± 0.00013
$\Omega_{\mathrm{cdm}} h^2$	0.11872 ± 0.00095	0.11864 ± 0.00098	0.11869 ± 0.00093	0.11856 ± 0.00096
$100\theta_s$	1.04200 ± 0.00029	1.04202 ± 0.00028	1.04200 ± 0.00029	1.04201 ± 0.00028
$\ln\left(10^{10} A_s\right)$	3.041 ± 0.016	3.041 ± 0.016	3.041 ± 0.016	3.042 ± 0.016
n_s	0.9686 ± 0.0037	0.9687 ± 0.0039	0.9685 ± 0.0036	0.9690 ± 0.0037
τ_{reio}	0.0543 ± 0.0078	0.0540 ± 0.0080	0.0541 ± 0.0077	0.0545 ± 0.0076
$10^{-4}\alpha$	$-$	< 2.67	< 5.73	$-$
λ	$-$	< 0.109	< 0.109	< 0.406
ϕ_{ini}	$-$	$1.0004^{+0.0078}_{-0.0089}$	$-$	$-$
z_{reio}	7.63 ± 0.79	7.60 ± 0.82	7.61 ± 0.77	7.64 ± 0.77
Y_{He}	0.247881 ± 0.000056	0.247882 ± 0.000056	0.247880 ± 0.000056	0.247885 ± 0.000057
H_0	67.98 ± 0.42	68.02 ± 0.44	67.99 ± 0.42	$67.67^{+0.56}_{-0.45}$
M	-19.410 ± 0.012	-19.409 ± 0.012	-19.410 ± 0.012	-19.415 ± 0.013
σ_8	0.8057 ± 0.0069	0.8066 ± 0.0071	0.8067 ± 0.0068	$0.8019^{+0.0080}_{-0.0072}$
$\Delta\chi^2_{\min}$	$-$	$+2.54$	$+1.46$	$+1.56$
$\ln B_{i,\Lambda\mathrm{CDM}}$	$-$	-9.29	-4.13	-1.39

Table 2. Observational constraints at a 68% confidence level on the independent and derived cosmological parameters for the ΛCDM, IDE, IDE with fixed ϕ_{ini}, and uncoupled quintessence models using PL18+BAO+Pantheon+CC+RSD. The quantities in the second half of this table are the derived parameters of our analysis which are the redshift of reionisation z_{reio}, the Helium fraction Y_{He}, the Hubble constant H_0, the absolute magnitude of SN1a as inferred from the data sets used M, and the present day mass fluctuation amplitude at $8h^{-1}\,\mathrm{Mpc}$ σ_8.

outlined below. In addition to this, the `GetDist`[3] [35] Python package is used to analyse the chains and produce the values and plots of the parameters in table 2 and in figures 4 to 6. Furthermore, we report the difference between the best-fit χ^2 value for a model i with respect to ΛCDM, $\Delta\chi^2_{\min} = \chi^2_{\min,\mathrm{i}} - \chi^2_{\min,\Lambda\mathrm{CDM}}$, in table 2. Finally, we calculate the Bayes factor of a scalar field model with respect to the ΛCDM model, $B_{i,\Lambda\mathrm{CDM}}$, by using the `MCEvidence`[4] code [36]. The natural logarithm of this Bayes factor, $\ln B_{i,\Lambda\mathrm{CDM}}$, is shown in the last row of table 2.

---

[3]https://github.com/cmbant/getdist.
[4]https://github.com/yabebalFantaye/MCEvidence.
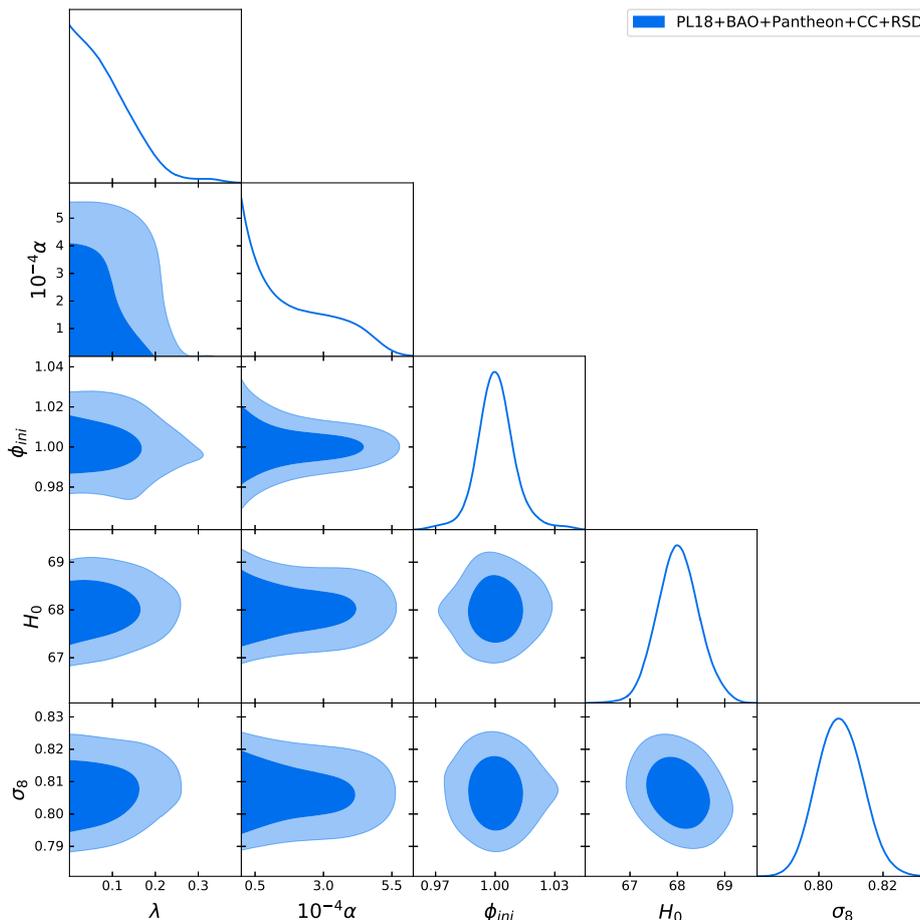
Figure 4. 2D marginalised posterior distributions for the IDE model using the PL18+BAO+Pantheon+CC+RSD data-set.

We use the following combination of recent observational data sets in order to analyse and constrain the IDE model:

- Cosmic Microwave Background:

  We use the TTTEEE+lowE Cosmic Microwave Background (CMB) likelihood from the Planck 2018 release [29, 37]. This includes temperature (TT) and polarisation (EE) anisotropy data as well as cross-correlation data between temperature and polarisation (TE) at high and low multipoles.

- Baryon Acoustic Oscillations:

  We consider Baryon Acoustic Oscillations (BAO) measurements coming from BOSS DR12 [38], 6dFGS [39], and SDSS-MGS [40] for use in our analysis.

- Type Ia Supernovae:

  We use the Pantheon data catalog consisting of 1048 points in the region $z \in [0.01, 2.3]$ of SNIa luminosity distance data as provided by [41].
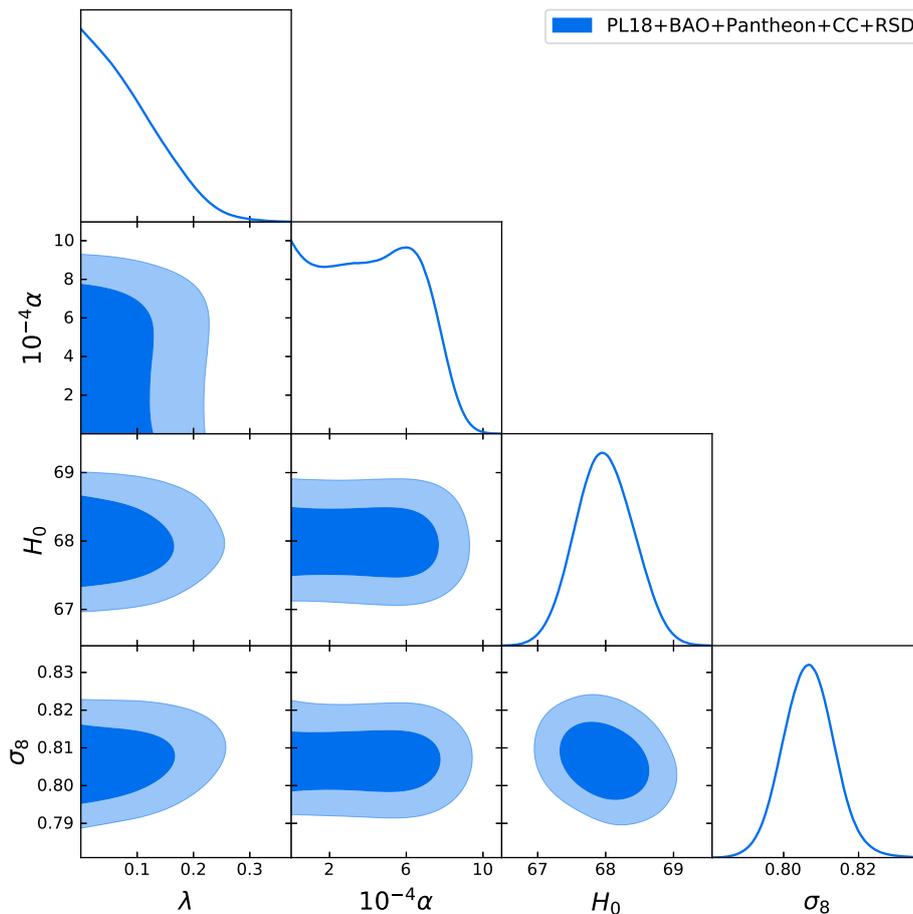
Figure 5. 2D marginalised posterior distributions for the IDE($\phi_{\text{ini}} = 1M_{\text{Pl}}$) model using the PL18+ BAO+Pantheon+CC+RSD data-set.

- Redshift Space Distortions:

  We employ the 'Gold 2018' Redshift Space Distortions (RSD) data set compilation consisting of 22 measurements as described in [42] and a likelihood code as detailed in [43].

- Cosmic Chronometers:

  We use 31 measurements of $H(z)$ from cosmic chronometers (CC) in the redshift range $z \in [0.07, 1.965]$ as detailed in table 4 of [44].

The results for our data analysis are shown in table 2 where we compare constraints of the ΛCDM, IDE, IDE with fixed ϕ_{ini}, and uncoupled quintessence models using the full PL18+BAO+Pantheon+CC+RSD data set for all models; in figure 4 where we display the 2D marginalised posterior distributions for parameters in the IDE model; in figure 5 where we display the 2D marginalised posterior distributions for parameters in the IDE ($\phi_{\text{ini}} = 1M_{\text{Pl}}$) model; and in figure 6 where we present the 1D marginalised posterior distribution for ϕ_{ini} in the IDE model. We utilise the full PL18+BAO+Pantheon+CC+RSD data set in all cases in order to obtain convergence for all the models, with all parameters achieving $|R-1| < 0.03$, where R is the Gelman-Rubin statistic [45]. Since attractor mechanisms drive the field
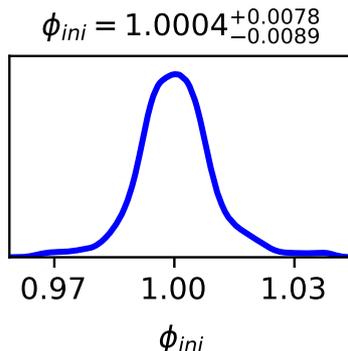
Figure 6. 1D marginalised posterior distribution for ϕ_{ini} in the IDE model using the PL18+BAO+Pantheon+CC+RSD data-set.

towards the minimum of the coupling function in the early universe, we investigate the case where the initial value of the scalar field sits directly at the minimum, i.e. when $\phi_{\text{ini}} = 1 M_{\text{Pl}}$, in this paper. In addition to ΛCDM and the IDE model, we also consider the uncoupled model (by imposing $\alpha = 0$) for comparison and to illustrate the impact of including the coupling on the parameter constraints. For the uncoupled model, owing to the form of the potential, we fix the initial value of the scalar field ϕ_{ini} and do not allow it to vary.

One of the first things to notice is the large values of the coupling constant α allowed by the data for the IDE models as can be seen in figures 4 and 5. We obtain an upper limit for α in both cases, of $10^{-4}\alpha < 2.67$ at 1σ for the IDE model and $10^{-4}\alpha < 5.73$ at 1σ for the IDE ($\phi_{\text{ini}} = 1 M_{\text{Pl}}$) model. In the case where the field initially sits at the minimum, the model only differs from an uncoupled quintessence model at late-times $z \lesssim 1$, whereas in the case where the initial field value is allowed to vary, the IDE model can differ significantly from an uncoupled quintessence model both at late-times and at earlier times since the magnitude of the coupling β depends on α and the distance between the field and minimum ϕ_* (eq. (2.5)). This early-time deviation can have a pronounced effect on cosmological observables, such as the matter power spectrum, as can be seen in the lower panel of figure 3, and hence the coupling constant α is more readily constrained in our analysis when ϕ_{ini} is allowed to vary.

Using the best-fit values for the cosmological parameters derived from the IDE models and the upper 1σ limits for scalar field parameters α and λ, as displayed in table 2, we can infer an upper limit on the present-day dark sector coupling of $\beta \approx 0.30$ and $\beta \approx 0.29$ for the IDE and IDE ($\phi_{\text{ini}} = 1 M_{\text{Pl}}$) models respectively. Note that the two IDE models have a similar coupling strength β at present-day despite the IDE ($\phi_{\text{ini}} = 1 M_{\text{Pl}}$) model allowing for larger values of coupling constant α. This is because the fifth-force depends not only on α, but also on the distance traversed by the field from the minimum ϕ_*, which is in turn determined by the values of the cosmological parameters. In particular, we recall that increasing α causes the motion of the field to slow down at late-times, such that increasing α does not have as significant an impact on the fifth-force as, say, increasing the steepness of the scalar field potential, λ, as can be seen in figure 2.

These upper limits on the coupling strengths correspond to upper limits on the present-day dark sector fifth-force that is $\sim 18\%$ the strength of gravity in the IDE and IDE ($\phi_{\text{ini}} = 1 M_{\text{Pl}}$) models. This is in stark contrast to the widely-studied IDE models where the coupling β between DE and DM is assumed to be constant, in which case the strength of the fifth-force is constrained to be $< 1\%$ the strength of gravity [16]. This result shows that once

the assumption of a constant coupling β is relaxed, and hence the coupling β is allowed to be dynamical in nature and variable with time, cosmological observations at the background and linear perturbation level do not constrain the fifth-force so stringently, allowing for the dark sector fifth-force to potentially be quite strong.

We obtain an upper limit on the slope of the potential of $\lambda < 0.109$ at 1σ for the IDE models and an upper limit of $\lambda < 0.406$ at 1σ for the uncoupled quintessence model. We can see that this IDE model does not help to alleviate the swampland requirement of $|V'/V| \geq c \sim \mathcal{O}(1)$ and in fact exacerbates the tension when compared to the uncoupled model for this data set combination.

In figure 4, we see that for the IDE model where $\phi_{\rm ini}$ is allowed to vary, there exists a negative correlation between the conformal coupling constant, α, and slope of the scalar field potential, λ. The same value of σ_8 can be achieved with a large value of α and small value of λ and vice versa, hence a degeneracy arises between these two parameters with the inclusion of RSD data. This degeneracy does not exist when $\phi_{\rm ini}$ is set to the minimum of the coupling function, as can be seen in figure 5, since there is no early-time enhancement of $G_{\rm eff}$ causing an increase in σ_8, and so increasing α results in only a minimal increase in σ_8 in these models, due to late-time effects alone.

We justify the prior for the initial value of the scalar field, $\phi_{\rm ini}$, to be centred about the minimum of the conformal coupling function owing to the attractor mechanisms afore-mentioned. We allow $\phi_{\rm ini}$ to vary as a cosmological parameter in our analysis for the IDE model and find that it is tightly constrained about the minimum of the coupling function, with a mean of $\phi_{\rm ini}/M_{\rm Pl} = 1.0004^{+0.0078}_{-0.0089}$ at 1σ as in figure 6, in agreement with the attractor mechanisms discussed in [21].

In table 2, we see that despite the uncoupled quintessence and IDE models introducing extra degrees of freedom, $\Delta\chi^2_{\rm min} > 0$ for all the models, indicating a worse fit than ΛCDM for this particular data-set combination. Furthermore, we see that $\ln B_{i,\Lambda\rm CDM} < 0$ for both the coupled and uncoupled models. According to Jeffrey's scale [46], this indicates that ΛCDM is 'very strongly' preferred over the IDE model, 'strongly' preferred over the IDE ($\phi_{\rm ini} = 1M_{\rm Pl}$) model and 'definitely' preferred over the uncoupled quintessence model. Despite the IDE ($\phi_{\rm ini} = 1M_{\rm Pl}$) model possessing a less positive $\Delta\chi^2_{\rm min}$ than the uncoupled quintessence model, thus indicating a better fit, this is not offset by the introduction of the extra parameter α, and so the Bayesian evidence $\ln B_{i,\Lambda\rm CDM}$ is more negative for this model.

4 Summary and conclusions

In this paper we have studied a specific IDE model, in which a fifth force between DM particles switches on at the onset of DE domination. This is achieved by considering a coupling function which possesses a minimum at a certain field value ϕ_*. The DE field evolves away from the minimum due to the influence of the potential energy. In contrast to other interacting DE models, the fifth force between DM particles becomes important only at the end of matter domination, if the field does sit at the minimum of the coupling function initially. We used several data sets to constrain $\phi_{\rm ini}$, the coupling parameter α and the slope of the potential energy λ.

Our main findings can be summarised as follows:

- The initial value of the field, deep inside the radiation dominated epoch, is constrained to be very near the minimum of the coupling function.

- The constraint on λ is weaker for the uncoupled model ($\lambda < 0.406$) than in the IDE models ($\lambda < 0.109$).

- The coupling parameter α is only weakly constrained ($10^{-4}\alpha \lesssim 2.7$ at 1σ for the IDE model and $10^{-4}\alpha \lesssim 5.7$ at 1σ for the IDE ($\phi_{\text{ini}} = 1M_{\text{Pl}}$) model).

- Since the effective coupling depends also on the value of the DE field ϕ, the effective gravitational constant is determined by the dynamics of DE and hence by both α and λ. The dependence of the effective gravitational coupling on λ and α is illustrated in figure 2.

Whilst Bayesian model selection analysis indicates that the IDE model considered is not preferred over ΛCDM, our study shows that equivalence principle violations in the dark sector at the present epoch are much less constrained than previously thought. This is because such new interactions may result from the dynamics of DE itself and only become important late in cosmic history. The data sets used in this paper, which measure the evolution of the cosmological background and cosmological perturbations at the linear level, do not constrain the fifth force strongly and the model is, for a wide range of parameters, indistinguishable from the ΛCDM model. We do expect the model to differ from ΛCDM at much smaller length scales, for which linear perturbation theory is no longer adequate. The fifth force is likely to leave an imprint on the evolution of non-linear perturbations and affect, for example, the matter power spectra on small scales. It would also be interesting to study the tidal tail test [47] in this model, since the coupling switches on only at late times. We do expect this test to constrain this model further. We leave these studies for future work.

Acknowledgments

References

[1] S. Weinberg, *The Cosmological Constant Problem*, *Rev. Mod. Phys.* **61** (1989) 1 [INSPIRE].

[2] T. Padmanabhan, *Cosmological constant: The Weight of the vacuum*, *Phys. Rept.* **380** (2003) 235 [hep-th/0212290] [INSPIRE].

[3] J. Martin, *Everything You Always Wanted To Know About The Cosmological Constant Problem (But Were Afraid To Ask)*, *C R Phys.* **13** (2012) 566 [arXiv:1205.3365] [INSPIRE].

[4] E. Abdalla et al., *Cosmology intertwined: A review of the particle physics, astrophysics, and cosmology associated with the cosmological tensions and anomalies*, *JHEAp* **34** (2022) 49 [arXiv:2203.06142] [INSPIRE].

[5] N. Schöneberg, G. Franco Abellán, A. Pérez Sánchez, S.J. Witte, V. Poulin and J. Lesgourgues, *The H0 Olympics: A fair ranking of proposed models*, *Phys. Rept.* **984** (2022) 1 [arXiv:2107.10291] [INSPIRE].

[6] E. Di Valentino et al., *In the realm of the Hubble tension—a review of solutions*, *Class. Quant. Grav.* **38** (2021) 153001 [arXiv:2103.01183] [INSPIRE].

[7] C. Wetterich, *Cosmology and the Fate of Dilatation Symmetry*, *Nucl. Phys. B* **302** (1988) 668 [arXiv:1711.03844] [INSPIRE].

[8] B. Ratra and P.J.E. Peebles, *Cosmological Consequences of a Rolling Homogeneous Scalar Field*, *Phys. Rev. D* **37** (1988) 3406 [INSPIRE].

[9] R.R. Caldwell, R. Dave and P.J. Steinhardt, *Cosmological imprint of an energy component with general equation of state*, *Phys. Rev. Lett.* **80** (1998) 1582 [astro-ph/9708069] [INSPIRE].

[10] V. Poulin, T.L. Smith, T. Karwal and M. Kamionkowski, *Early Dark Energy Can Resolve The Hubble Tension*, *Phys. Rev. Lett.* **122** (2019) 221301 [arXiv:1811.04083] [INSPIRE].

[11] M. Braglia, M. Ballardini, F. Finelli and K. Koyama, *Early modified gravity in light of the H_0 tension and LSS data*, *Phys. Rev. D* **103** (2021) 043528 [arXiv:2011.12934] [INSPIRE].

[12] S.M. Carroll, *Quintessence and the rest of the world*, *Phys. Rev. Lett.* **81** (1998) 3067 [astro-ph/9806099] [INSPIRE].

[13] C. Wetterich, *The Cosmon model for an asymptotically vanishing time dependent cosmological 'constant'*, *Astron. Astrophys.* **301** (1995) 321 [hep-th/9408025] [INSPIRE].

[14] L. Amendola, *Coupled quintessence*, *Phys. Rev. D* **62** (2000) 043511 [astro-ph/9908023] [INSPIRE].

[15] G.R. Farrar and P.J.E. Peebles, *Interacting dark matter and dark energy*, *Astrophys. J.* **604** (2004) 1 [astro-ph/0307316] [INSPIRE].

[16] C. Van De Bruck and J. Mifsud, *Searching for dark matter - dark energy interactions: going beyond the conformal case*, *Phys. Rev. D* **97** (2018) 023506 [arXiv:1709.04882] [INSPIRE].

[17] M. Archidiacono, E. Castorina, D. Redigolo and E. Salvioni, *Unveiling dark fifth forces with linear cosmology*, *JCAP* **10** (2022) 074 [arXiv:2204.08484] [INSPIRE].

[18] G. Obied, H. Ooguri, L. Spodyneiko and C. Vafa, *De Sitter Space and the Swampland*, arXiv:1806.08362 [INSPIRE].

[19] P. Agrawal, G. Obied, P.J. Steinhardt and C. Vafa, *On the Cosmological Implications of the String Swampland*, *Phys. Lett. B* **784** (2018) 271 [arXiv:1806.09718] [INSPIRE].

[20] E. Palti, *The Swampland: Introduction and Review*, *Fortsch. Phys.* **67** (2019) 1900037 [arXiv:1903.06239] [INSPIRE].

[21] C. van de Bruck and C.C. Thomas, *Dark energy, the swampland, and the equivalence principle*, *Phys. Rev. D* **100** (2019) 023515 [arXiv:1904.07082] [INSPIRE].

[22] P. Agrawal, G. Obied and C. Vafa, *H_0 tension, swampland conjectures, and the epoch of fading dark matter*, *Phys. Rev. D* **103** (2021) 043523 [arXiv:1906.08261] [INSPIRE].

[23] Y. Olguin-Trejo, S.L. Parameswaran, G. Tasinato and I. Zavala, *Runaway Quintessence, Out of the Swampland*, *JCAP* **01** (2019) 031 [arXiv:1810.08634] [INSPIRE].

[24] P. Brax, C. van de Bruck and A.-C. Davis, *Swampland and screened modified gravity*, *Phys. Rev. D* **101** (2020) 083514 [arXiv:1911.09169] [INSPIRE].

[25] B. Valeixo Bento, D. Chakraborty, S.L. Parameswaran and I. Zavala, *Dark Energy in String Theory*, *PoS* **CORFU2019** (2020) 123 [arXiv:2005.10168] [INSPIRE].

[26] M. Brinkmann, M. Cicoli, G. Dibitetto and F.G. Pedro, *Stringy multifield quintessence and the Swampland*, *JHEP* **11** (2022) 044 [arXiv:2206.10649] [INSPIRE].

[27] T. Damour and A.M. Polyakov, *The String dilaton and a least coupling principle*, *Nucl. Phys. B* **423** (1994) 532 [hep-th/9401069] [INSPIRE].

[28] P. Brax, C. van de Bruck, A.-C. Davis and D. Shaw, *The Dilaton and Modified Gravity*, *Phys. Rev. D* **82** (2010) 063519 [arXiv:1005.3735] [INSPIRE].

[29] PLANCK collaboration, *Planck 2018 results. VI. Cosmological parameters*, *Astron. Astrophys.* **641** (2020) A6 [arXiv:1807.06209] [*Erratum ibid.* **652** (2021) C4] [INSPIRE].

[30] L. Amendola, *Linear and non-linear perturbations in dark energy models*, *Phys. Rev. D* **69** (2004) 103524 [astro-ph/0311175] [INSPIRE].

[31] J. Lesgourgues, *The Cosmic Linear Anisotropy Solving System (CLASS) I: Overview*, arXiv:1104.2932 [INSPIRE].

[32] D. Blas, J. Lesgourgues and T. Tram, *The Cosmic Linear Anisotropy Solving System (CLASS) II: Approximation schemes*, *JCAP* **07** (2011) 034 [arXiv:1104.2933] [INSPIRE].

[33] T. Brinckmann and J. Lesgourgues, *MontePython 3: boosted MCMC sampler and other features*, *Phys. Dark Univ.* **24** (2019) 100260 [arXiv:1804.07261] [INSPIRE].

[34] B. Audren, J. Lesgourgues, K. Benabed and S. Prunet, *Conservative Constraints on Early Cosmology: an illustration of the Monte Python cosmological parameter inference code*, *JCAP* **02** (2013) 001 [arXiv:1210.7183] [INSPIRE].

[35] A. Lewis, *GetDist: a Python package for analysing Monte Carlo samples*, arXiv:1910.13970 [INSPIRE].

[36] A. Heavens et al., *Marginal Likelihoods from Monte Carlo Markov Chains*, arXiv:1704.03472 [INSPIRE].

[37] PLANCK collaboration, *Planck 2018 results. V. CMB power spectra and likelihoods*, *Astron. Astrophys.* **641** (2020) A5 [arXiv:1907.12875] [INSPIRE].

[38] BOSS collaboration, *The clustering of galaxies in the completed SDSS-III Baryon Oscillation Spectroscopic Survey: cosmological analysis of the DR12 galaxy sample*, *Mon. Not. Roy. Astron. Soc.* **470** (2017) 2617 [arXiv:1607.03155] [INSPIRE].

[39] F. Beutler et al., *The 6dF Galaxy Survey: Baryon Acoustic Oscillations and the Local Hubble Constant*, *Mon. Not. Roy. Astron. Soc.* **416** (2011) 3017 [arXiv:1106.3366] [INSPIRE].

[40] A.J. Ross, L. Samushia, C. Howlett, W.J. Percival, A. Burden and M. Manera, *The clustering of the SDSS DR7 main Galaxy sample — I. A 4 per cent distance measure at $z = 0.15$*, *Mon. Not. Roy. Astron. Soc.* **449** (2015) 835 [arXiv:1409.3242] [INSPIRE].

[41] PAN-STARRS1 collaboration, *The Complete Light-curve Sample of Spectroscopically Confirmed SNe Ia from Pan-STARRS1 and Cosmological Constraints from the Combined Pantheon Sample*, *Astrophys. J.* **859** (2018) 101 [arXiv:1710.00845] [INSPIRE].

[42] B. Sagredo, S. Nesseris and D. Sapone, *Internal Robustness of Growth Rate data*, *Phys. Rev. D* **98** (2018) 083543 [arXiv:1806.10822] [INSPIRE].

[43] R. Arjona, J. García-Bellido and S. Nesseris, *Cosmological constraints on nonadiabatic dark energy perturbations*, *Phys. Rev. D* **102** (2020) 103526 [arXiv:2006.01762] [INSPIRE].

[44] M. Moresco et al., *A 6% measurement of the Hubble parameter at $z \sim 0.45$: direct evidence of the epoch of cosmic re-acceleration*, *JCAP* **05** (2016) 014 [arXiv:1601.01701] [INSPIRE].

[45] A. Gelman and D.B. Rubin, *Inference from Iterative Simulation Using Multiple Sequences*, *Statist. Sci.* **7** (1992) 457 [INSPIRE].

[46] R.E. Kass and A.E. Raftery, *Bayes Factors*, *J. Am. Statist. Assoc.* **90** (1995) 773 [INSPIRE].

[47] M. Kesden and M. Kamionkowski, *Tidal Tails Test the Equivalence Principle in the Dark Sector*, *Phys. Rev. D* **74** (2006) 083007 [astro-ph/0608095] [INSPIRE].